Influence of metallothionein-1 localization on its function

Marilyne LEVADOUX-MARTIN*[1], John E. HESKETH*[1], John H. BEATTIE* and Heather M. WALLACE†[2]

*Rowett Research Institute, Greenburn Road, Bucksburn, Aberdeen AB21 9SB, Scotland, U.K., and †Department of Medicine and Therapeutics and Biomedical Sciences, University of Aberdeen, Polwarth Building, Aberdeen AB25 2ZD, Scotland, U.K.

Metallothioneins (MTs) have a major role to play in metal metabolism, and may also protect DNA against oxidative damage. MT protein has been found localized in the nucleus during S-phase. The mRNA encoding the MT-1 isoform has a perinuclear localization, and is associated with the cytoskeleton; this targeting, due to signals within the 3′-untranslated region (3′-UTR), facilitates nuclear localization of MT-1 during S-phase [Levadoux, Mahon, Beattie, Wallace and Hesketh (1999) J. Biol. Chem. **274**, 34961–34966]. Using cells transfected with MT gene constructs differing in their 3′-UTRs, the role of MT protein in the nucleus has been studied. Chinese hamster ovary cells were transfected with either the full MT gene (MTMT cells) or with the MT 5′-UTR and coding region linked to the 3′-UTR of glutathione peroxidase (MTGSH cells). Cell survival following exposure to oxidative stress and chemical agents was higher in cells expressing the native MT gene than in cells where MT localization was disrupted, or in untransfected cells. Also, MTMT cells showed less DNA damage than MTGSH cells in response to either hydrogen peroxide or mutagen. After exposure to UV light or mutagen, MTMT cells showed less apoptosis than MTGSH cells, as assessed by DNA fragmentation and flow cytometry. The data indicate that the perinuclear localization of MT mRNA is important for the function of MT in a protective role against DNA damage and apoptosis induced by external stress.

Key words: apoptosis, DNA damage, mRNA localization, nuclear localization, oxidative stress.

INTRODUCTION

The appropriate localization of proteins within the cell is critical for cell organization and development. The localization of membrane-associated and secreted proteins, which are destined for specific compartments in the cell, is achieved by the presence of signals in their polypeptide chains [1,2], whereas cytosolic proteins can be targeted either by protein signals [3] or by the recently discovered mechanism of mRNA localization [4,5]. To date, the available evidence indicates that such mRNA localization to specific regions of the cell is due to targeting signals in their 3′-untranslated regions (3′-UTRs) [5,6]. Furthermore, although it was thought for many years that cytosolic proteins were translated on free polysomes, there is now evidence for an anchorage of polysomes to the cytoskeleton of the cell [5–8]. It has been suggested that this sorting of mRNAs could provide a mechanism by which proteins are localized close to their sites of function, and could therefore provide a critical mechanism in cell organization.

Some mRNAs are transported to the cell periphery, whereas others, including those encoding c-*myc* [9] and metallothionein (MT)-1 [10], are found in the perinuclear cytoplasm and are associated with the cytoskeleton. Neither the functional role of perinuclear mRNA localization nor the consequences of loss of localization have been defined.

MTs are a family of low-molecular-mass metal-binding protein isoforms. Although considered mainly cytoplasmic, MT has been found localized in the nucleus of the cell under different physiological conditions. For example, during the G_1-to-S-phase transition of the cell cycle or following metal toxicity, MT is found specifically in the nucleus [11–14]. The function of MT in the nucleus remains unclear, but it may play a role in protecting against metal toxicity and the harmful effects of oxidative stress (for a review, see [15]).

We have developed previously a transfected cell-culture model to study MT-1 mRNA localization and its role in protein distribution [14]. Chinese hamster ovary (CHO) cells were transfected with either the full-length MT-1 gene containing its endogenous 3′-UTR (MTMT cells) or the MT-1 5′-UTR and coding regions linked to the 3′-UTR of glutathione peroxidase (MTGSH cells). The cytosolic glutathione peroxidase 3′-UTR was chosen because this mRNA had previously been found in free polysomes, as opposed to cytoskeletal-bound polysomes [16], and therefore we expected this 3′-UTR not to contain a localization signal. Indeed, this change in MT-1 3′-UTR led to the delocalization of the mRNA, with a loss of perinuclear localization and association with the cytoskeleton found in the native MTMT transcripts [10]. Furthermore, delocalization of MT-1 mRNA led to the delocalization of MT-1 protein and, particularly, to the loss of localization of this protein in the nucleus of the cells during the early S-phase of their cell cycle [14].

In the present study, we used these same transfected cell lines to investigate the functional consequences of loss of perinuclear mRNA localization and the role of MT-1 in the nucleus. Our approach was to examine the role of MT-1 during oxidative stress and investigate the involvement of MT in protecting cells against DNA damage and apoptosis.

MATERIALS AND METHODS

Reagents

Diquat was a gift from Zeneca (Wilmington, DE, U.S.A.). 3-(4,5-Dimethylthiazol-2-yl)-2,5-diphenyl-2*H*-tetrazolium bromide

Abbreviations used: CHO, Chinese hamster ovary; FBS, fetal bovine serum; MNNG, *N*-methyl-*N*′-nitro-*N*-nitrosoguanidine; MT, metallothionein; MTGSH cells, CHO cells transfected with the MT-1 5′-UTR and coding regions linked to the 3′-UTR of glutathione peroxidase; MTMT cells, CHO cells transfected with the full-length MT-1 gene containing its endogenous 3′-UTR; MTT, 3-(4,5-dimethylthiazol-2-yl)-2,5-diphenyltetrazolium bromide; PI, propidium iodide; UTR, untranslated region.

[1] Present address: Department of Biological and Nutritional Sciences, University of Newcastle-upon-Tyne, Kings Road, Newcastle-upon-Tyne, U.K.
[2] To whom correspondence should be addressed (e-mail h.m.wallace@abdn.ac.uk).

(MTT), *N*-methyl-*N'*-nitro-*N*-nitrosoguanidine (MNNG), propidium iodide (PI) and DMSO were purchased from Sigma Chemical Co. (St Louis, MO, U.S.A.). The Suicide Track Kit was obtained from Calbiochem (La Jolla, CA, U.S.A.).

Transfected cell lines

Two of the transfected cell lines used for this work have been described previously [17]. Briefly, MTMT cells were obtained by transfection of CHO cells with a vector containing the MT-1 full-length gene inserted into the *Bam*HI/*Apa*I sites of the polylinker region of pcDNA3. MTGSH cells consisted of the 5′-UTR and coding region of the MT-1 gene linked to the 3′-UTR of glutathione peroxidase; this construct was inserted into the *Bam*HI/*Not*I sites of the polylinker region of pcDNA3. One clone for each cell line was chosen so that both clones expressed the same amount of MT-1 protein and could therefore be compared directly. The level of cellular MT that we selected was comparable with constitutive levels, which we have measured in rodent liver. The objective was to investigate the function of physiological levels of MT, rather than examining the effect of MT overexpression, which may perturb cellular metabolism independently of the toxic substances selected for study.

IDIGSH cells, a control cell line, were obtained by transfection of CHO cells with a plasmid IDIGSH, corresponding to the 5′-UTR and coding region of the deiodinase type 1 linked to the 3′-UTR of glutathione peroxidase [18], and were inserted into the *Bst*XI/*Not*I sites of the polylinker region of pcDNA3. After transfection, clones were selected and assayed for their glutathione peroxidase mRNA level; one clone was selected that had a glutathione peroxidase mRNA level similar to that of the MTGSH clone already chosen.

Cell culture and transfection

CHO cells (European Collection of Animal Cell Cultures no. 85050302) were grown in Ham's F-12 modified medium supplemented with sodium bicarbonate (1.176 g/l), 10 % (v/v) fetal bovine serum (FBS), penicillin (50 units/ml), streptomycin (50 μg/ml) and amphotericin B (Fungizone; 2.5 μg/ml) at 37 °C in an atmosphere of 5 % CO_2. When appropriate, cells were synchronized in the G_0 phase of the cell cycle by culture in 0.5 % (v/v) FBS for 48 h. After serum deprivation, cells were returned to S-phase by adding back medium containing 10 % (v/v) FBS. Synchronization was assessed by [^{3}H]thymidine incorporation [14]. Transfection of CHO cells was performed using LIPOFECTAMINE™. Clones were selected by addition of 6–18 μl/ml G418.

MTT assay

Exponentially growing cells were resuspended in fresh medium and were seeded into 96-well plates at a seeding density of 1.5×10^4 cells/cm^2. MTT assay was performed using the method of Mosmann [19]. Results shown are the means for four separate experiments.

Comet assay

Cells treated appropriately with stress-inducing agents were washed twice with PBS. The monolayer was detached using trypsin, and cells were collected and embedded in 1 % low-melting-point agarose. The comet assay was performed according to the method of Collins et al. [20].

In the case of exposure of cells synchronized in early S-phase to MNNG, the conditions used for the comet assay (40 μM MNNG for 24 h) had to be altered slightly from those used on unsynchronized cells. Indeed, it was impossible to expose the cells for 24 h to MNNG and still expect the cells to be in the S-phase of their cell cycle. Therefore it was decided to expose the cells to a higher concentration of the stress-inducing compound, but for a shorter time; hence, after synchronization, cells were incubated with 1 mM MNNG for 90 min at 37 °C; these parameters were consistent with earlier studies [12,21]. H_2O_2 treatment was carried out in the same conditions used for the study of DNA damage on unsynchronized cells; cells were exposed for 5 min to 150 μM H_2O_2.

Quantification of DNA damage was carried out using the Komet software. This image analysis program calculates the intensity of 4,6-diamidino-2-phenylindole ('DAPI') staining in the head and in the tail of the comet; the head represents the undamaged DNA, whereas the damaged DNA was accumulated in the tail of the comet. For each gel, 50 random cells were quantified in each replicate; cells had to be isolated from others and free of any fluorescent contaminant. A camera linked to the microscope captured the images for subsequent analysis.

Apoptosis

DNA fragmentation

After exposure to stress, cells left attached at the bottom of the dish were detached using trypsin, and then combined with cells floating in the medium; apoptosis was monitored using a Suicide-Track Kit. Cells were treated according to the manufacturer's instructions, leading to the isolation of apoptotic DNA from genomic DNA and other components of the cell. The fragments of apoptotic DNA were separated on a 1.5 % (w/v) agarose gel in 1 × TAE buffer [50 mM acetic acid/0.4 mM Tris/acetate (pH 7.2)/10 mM EDTA] and visualized by staining the gel with 0.5 μg/ml ethidium bromide. Cells that had undergone apoptosis showed a classic 'ladder' of fragmented DNA, with fragments corresponding to multimers of approx. 180–200 bp [22].

Analysis of DNA fragmentation by flow cytometry

For each cell line, 3×10^6 cells/ml were subcultured into 90-mm dishes and left to grow before use as control cells or prior to exposure to stress-inducing agents at specific concentrations, for times appropriate to whichever drug was added. Samples were analysed in triplicate. The method used for detection of apoptotic cells depended upon the degradation of DNA occurring during apoptosis. This DNA fragmentation can be detected by flow cytometry as cells with a sub-G_1 DNA content. Hence quantification of this sub-G_1 peak by flow cytometry allows the quantification of the number of apoptotic cells in a population of cells.

Detection of DNA fragmentation by flow cytometry was on the basis of the method of Nicoletti et al. [23]. Briefly, treated and non-treated cells were collected and washed once in PBS. Following fixation in 70 % (v/v) ethanol, DNA was extracted in 192 ml of 0.2 M Na_2HPO_4/8 ml of 0.1 M citric acid, before being stained for 30 min with PI at room temperature (2 μg of PI/ml PBS and 200 μg/ml DNase-free RNase A). PI staining of DNA from 15000 cells was monitored using a Becton–Dickinson FACS Calibur flow cytometer.

Statistical analysis

Means and standard errors were calculated from replicates within an experiment, and each experiment was repeated at least three times. Groups were compared using ANOVA; this test is

based on the assumption that the populations have equal variance. This parameter was checked using Bartlett's test. When significant differences were found using ANOVA, a post-test was carried out: Bonferroni's multiple comparison test was used to compare several groups together, whereas Dunnett's test was used to compare single groups with a control group.

RESULTS

Cell survival using the MTT assay

Three of the cell lines used for this study have been described previously [14]. They consisted of native CHO cells (which have a low constitutive level of MT expression) and transfected CHO cells expressing either the 5′-UTR, coding region and 3′-UTR of the MT-1 gene (MTMT cells) or an MT-1 gene in which the endogenous 3′-UTR had been replaced by that from glutathione peroxidase (MTGSH cells). As shown previously and in Figure 1, the distribution of MT was different in the two cell lines. Immunocytochemistry showed that, in unsynchronized MTMT cells, MT-1 was localized around the nucleus, whereas in MTGSH cells it was distributed throughout the cytoplasm with no specific localization. When MTMT cells were synchronized in S-phase of the cell cycle, MT-1 was found concentrated in the nucleus; this did not occur in synchronized MTGSH cells.

Clones were isolated for each cell line and one clone per cell line was chosen so that the two clones would express the same amount of MT protein (150 ng/mg of total protein, which is approx. 7-fold higher than in the untransfected CHO cells). Measurement of MT content in the cells was performed by radioimmunoassay. In addition, a fourth CHO cell line not expressing MT, but expressing deiodinase linked to the glutathione peroxidase 3′-UTR [18], was used as a further control.

Cells were exposed to different doses of three stress-inducing compounds for 24 h. Cadmium chloride (Figure 2A) and the alkylating agent, MNNG (Figure 2B), were used at concentrations ranging from 0 to 100 μM and the herbicide, diquat (Figure 2C), at concentrations ranging from 0 to 400 μM. For each cell line, the inhibitory concentration that affects 50% of the cell population (IC_{50}) was derived from the survival curves (Table 1).

The IC_{50} obtained for each cell line revealed, in the three cases, a statistically higher resistance of the MTMT cells in response to stress compared with the three other cell lines (Table 1). MTMT cells were significantly more resistant ($P < 0.01$) to stress than the wild-type CHO cells and, moreover, were more resistant ($P < 0.05$) than the MTGSH cells. However, no statistical difference was found between MTGSH cells and the parental CHO cells. Furthermore, the IDIGSH cells behaved in a similar way to the wild-type CHO cells, showing that neither the transfection step nor the overexpression of the 3′-UTR of glutathione peroxidase modulated the response of the cells to stress (Table 1).

DNA damage

DNA damage in both wild-type and transfected CHO cells was then assessed in response to two different stress-inducing compounds, MNNG and hydrogen peroxide. The alkylating agent, MNNG, which is responsible for direct DNA damage by formation of single-strand breaks, was used at a concentration of 40 μM, a value close to the IC_{50} for all cell lines (Figure 2B). Cells

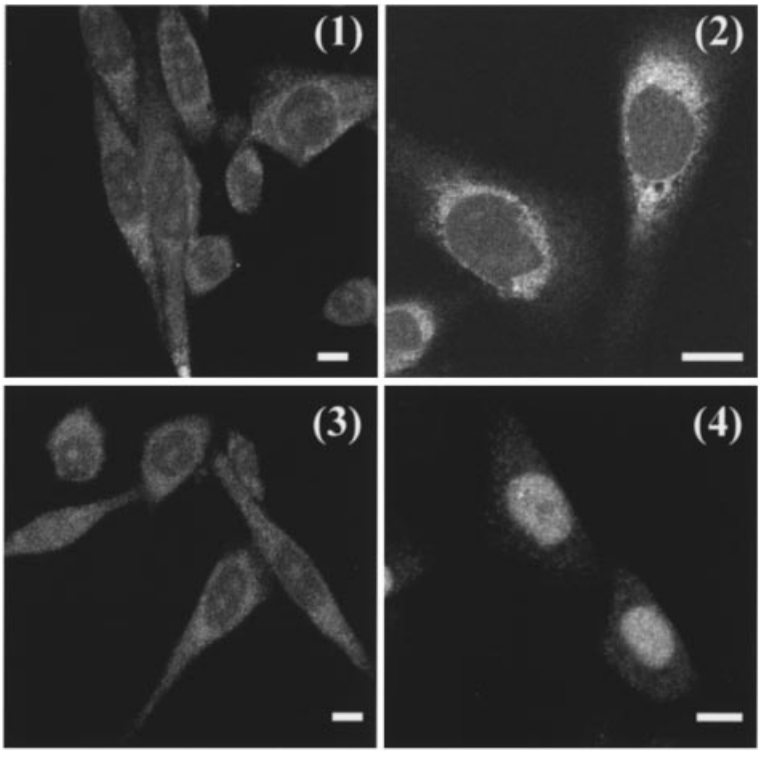

Figure 1 Confocal microscopy of MT distribution in exponentially growing transfected CHO cells and transfected CHO cells synchronized in S-phase

Sections (0.5 μm) through MTGSH (**1**) and MTMT (**2**) cells in exponentially growing populations of cells show a perinuclear localization of MT-1 in MTMT cells, but not in MTGSH cells; 0.5 μm sections through MTGSH (**3**) and MTMT (**4**) cells synchronized in S-phase show in a nuclear localization of MT-1 in MTMT cells and a cytoplasmic localization of MT-1 in MTGSH cells. Bars represent 10 μm.

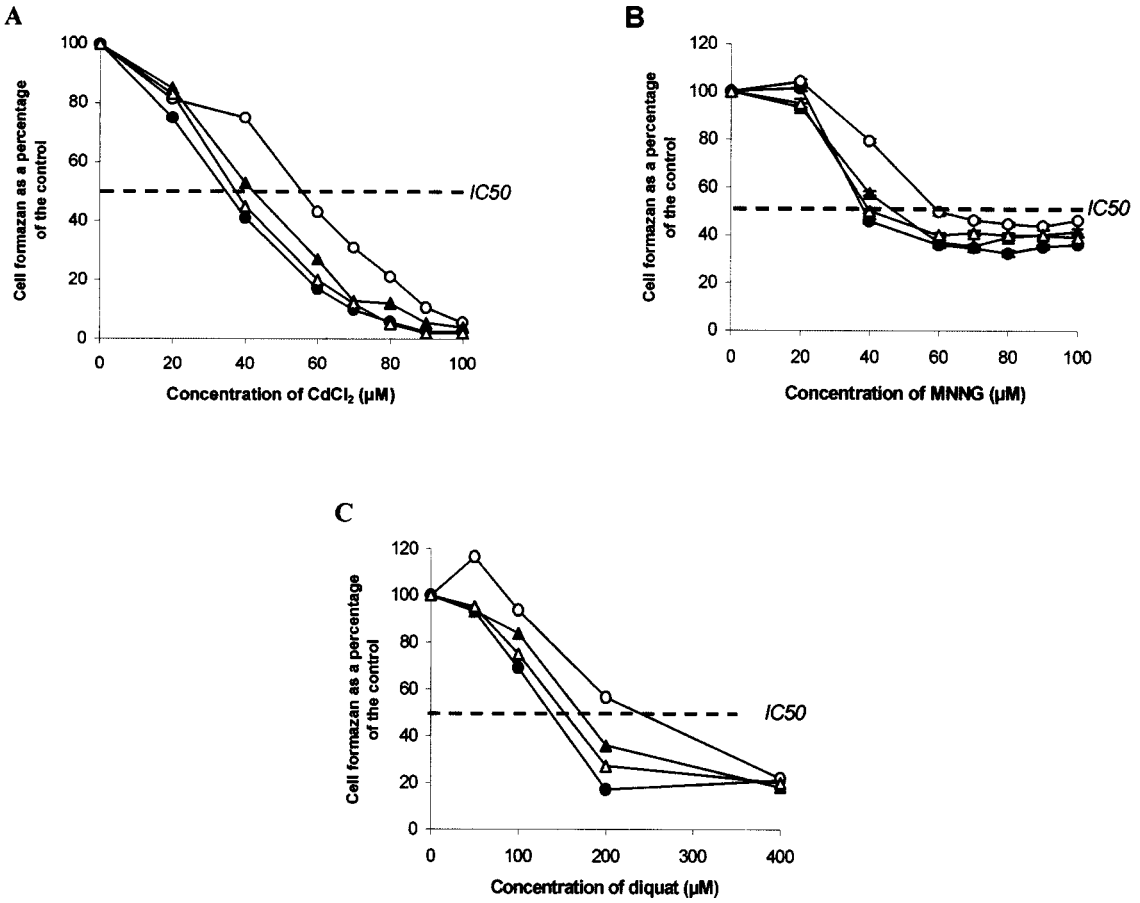

Figure 2 Cell survival after exposure to stress-inducing compounds

Untransfected CHO cells (●) and transfected cells (MTMT, ○; MTGSH, ▲; IDIGSH, △) were exposed to a range of concentrations of cadmium chloride (**A**), MNNG (**B**) or diquat (**C**). The percentage of surviving cells was calculated as a ratio of the absorbance of treated cells to that of the untreated control. Values shown are the means from three different experiments, each representing the mean for six samples.

Table 1 IC_{50} values after induction of stress

IC_{50} values were derived from the 'surviving' curves from each experiment. Results (means ± S.E.M.) are from four experiments, with six replicates per experiment. *Significant difference ($P < 0.05$) between MTMT cells and MTGSH cells; †indicates significant difference ($P < 0.01$) between MTMT and CHO cells, measured using Dunnett's test.

	IC_{50} values after exposure to stress (μM)		
Cell lines	$CdCl_2$	MNNG	Diquat
CHO	35.3 ± 4.0	37.7 ± 2.6	123.3 ± 7.8
MTMT	54.4 ± 6.0*†	60.7 ± 2.3*†	230.0 ± 10.3*†
MTGSH	40.3 ± 6.0	48.0 ± 2.1	167.3 ± 2.1
IDIGSH	36.1 ± 3.2	40.0 ± 1.2	145.0 ± 7.7

were incubated with the stress-inducer for 24 h, in order to make direct comparisons with the MTT assay.

The second stress-inducer used was hydrogen peroxide. This compound does not induce DNA damage by direct chemical attack of the molecule, but can create DNA damage via the formation of $OH^{\bullet}$ radicals by the Fenton and/or Haber–Weiss reactions, which can subsequently attack DNA. Alternatively, it can lead to the formation of $OH^{\bullet}$ radicals, which trigger a series of events that can activate nuclease enzymes that are capable of cleaving the DNA backbone. These two phenomena can act together in the cell. In these experiments, cells were exposed to 150 μM H_2O_2 for 5 min at 4 °C, to be consistent with previous studies [24].

When the comet assay was performed on exponentially growing cells (unsynchronized), the response of the three cell lines to both H_2O_2 and MNNG showed statistically significant increases in the amount of degraded DNA in the treated cells compared with their corresponding controls (Table 2). However, there was a significantly lower proportion of degraded DNA in both MTMT and MTGSH cells compared with the CHO wild-type cells ($P < 0.001$), and the MTMT cells showed significantly less DNA degradation ($P < 0.001$) than the MTGSH cells.

Since MT is found in the nucleus in S-phase [11,12,14], it was particularly important to assess DNA damage during this part of the cell cycle. When cells were synchronized in early S-phase, treatment with either MNNG or H_2O_2 caused a significant increase in DNA damage ($P < 0.01$) in each of the three cell lines compared with their respective synchronized controls (Table 2). Also, there was a statistically significant lower proportion of degraded DNA in both MTMT cells and MTGSH cells compared with CHO wild-type cells ($P < 0.001$); finally, MTMT cells

Table 2 DNA damage in unsynchronized and synchronized cells after exposure to H_2O_2 or MNNG

Results (shown as means ± S.E.M.) are expressed as a percentage of DNA in the tail of the comet (damaged DNA), and are from four experiments, each representing the analysis of 50 random cells per cell line. *Indicates significant difference ($P < 0.01$) between each treated cell line compared with its corresponding control, using Dunnett's test; †indicates significantly less damage ($P < 0.001$) in both MTMT cells and MTGSH cells compared with CHO cells, using Dunnett's test; ‡indicates statistically less damage ($P < 0.001$) in MTMT cells compared with MTGSH cells.

	DNA damage in cells (%)					
	Unsynchronized cells			Synchronized cells		
Cell lines	Control	H_2O_2	MNNG	Control	H_2O_2	MNNG
CHO	7.8 ± 1.2	61.6 ± 1.6*	88.8 ± 1.1*	7.9 ± 2.2	62.1 ± 2.2*	83.4 ± 4.0*
MTMT	7.9 ± 2.2	25.4 ± 1.6*†‡	57.8 ± 3.2*†‡	7.7 ± 1.8	18.4 ± 1.6*†‡	44.9 ± 5.1*†‡
MTGSH	8.6 ± 1.1	55.7 ± 3.0*†	84.3 ± 2.1*†	7.9 ± 2.0	50.5 ± 2.9*†	81.1 ± 2.1*†

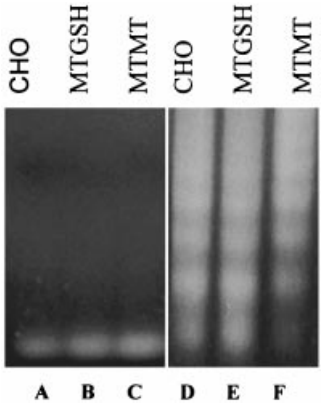

Figure 3 Agarose-gel analysis of DNA fragmentation after exposure to MNNG

Cells were exposed to 40 μM MNNG for 24 h. Lanes A–C, untreated cells; lanes D–F, MNNG-treated cells.

Table 3 Measurement of apoptosis following exposure to UVC light and MNNG

Values (means ± S.E.M.) expressed are shown as percentages of cells in the sub-G_1 peak, and represent the mean for four experiments. *Significant difference ($P < 0.01$) between MTMT as compared with the three other cell lines using Bonferroni's test.

	Percentage of cells in sub-G_1 peak after induction of stress			
Cell lines	Control	UVC light + 16 h	UVC light + 20 h	MNNG (40 μM)
CHO	0.7 ± 0.1	71.1 ± 5.9	77.6 ± 2.2	54.6 ± 6.0
MTMT	0.6 ± 0.1	45.2 ± 4.5*	50.3 ± 3.5*	35.9 ± 3.2*
MTGSH	0.6 ± 0.1	61.9 ± 3.5	61.4 ± 5.4	52.9 ± 1.4
IDIGSH	0.5 ± 0.3	68.9 ± 3.2	70.7 ± 3.5	55.1 ± 3.6

exhibited less damage after exposure to stress than MTGSH cells ($P < 0.01$).

Comparison of cells after exposure to MNNG and H_2O_2 revealed that there was no statistical difference in the amount of DNA damage between unsynchronized and synchronized parental CHO cells. Similarly, there was no difference when unsynchronized and synchronized MTGSH cells were compared. However, there was a significant reduction using MNNG ($P < 0.001$) and using H_2O_2 ($P < 0.05$) in DNA damage in synchronized MTMT cells compared with the unsynchronized cultures. These data indicate that the protective effect of MT-1 was most effective in S-phase.

Overall, these data suggest that MT can protect DNA from attack by free radicals, since both MTMT and MTGSH cells exhibited less damage than the CHO wild type. Moreover, comparison between the two transfected cell lines indicates that delocalization of MT leads to an increase in DNA damage. In the last part of these studies, we addressed whether these differences were reflected in the extent of apoptotic cell death.

Induction of apoptosis using UVC light and MNNG

CHO, MTMT and MTGSH cells were exposed to 20 J/m² UVC light and left to grow for up to 24 h before assessment of apoptosis by DNA fragmentation [22]. For up to 12 h after radiation of the cells, no DNA fragmentation could be seen in any of the four cell lines. However, after 16, 20 and 24 h incubation, all the cell lines exhibited 'laddering' of their DNA. In every case, there was less fragmentation in the MTMT cell line compared with the other two cell lines. The average size difference between the DNA fragments constituting the 'ladder' was approx. 180 bp (results not shown).

In further experiments, cells were exposed to 40 μM MNNG for 24 h and analysed for DNA fragmentation. No fragmentation of DNA could be seen in the untreated cells (Figure 3). However, the MNNG-treated cells displayed 'laddering' of their DNA under these stress conditions. The fragmentation pattern was consistent with the molecular mass expected (multimers of 180 bp) to result from the internucleosomal cleavage of DNA associated with apoptosis, indicating that after exposure of CHO untransfected and transfected cell lines to 40 μM MNNG for 24 h, cells were undergoing apoptosis. No clear-cut differences were seen between the 'ladders' of CHO and MTGSH cells; however, MTMT cells possessed less fragmented DNA.

The extent of apoptosis was quantified in the different cell lines by measurement of the sub-G_1 peak in the DNA flow-cytometric profiles. The percentage of cells undergoing apoptosis in untreated populations was similar in all four cell lines (MTMT, MTGSH, CHO and IDIGSH) and was close to zero. However, all cell lines underwent apoptosis after exposure to UVC light (Table 3). There was significantly less apoptosis ($P < 0.01$) in MTMT cells at 16 or 20 h after treatment with UVC than in the other cell lines (MTGSH, IDIGSH and the parental CHO cells). However, the number of apoptotic cells among MTGSH cells was significantly less ($P < 0.05$) following the same treatment compared with CHO and IDIGSH cells. After exposure of the

cells to 40 μM MNNG, there was statistically less apoptosis ($P < 0.01$) in MTMT cells than in the three other cell lines. MTGSH cells again showed significantly less apoptosis ($P < 0.05$) than both CHO and IDIGSH cell lines. There was no significant difference between CHO cells and IDIGSH cells in terms of the number of apoptotic cells following treatment with either UVC light or MNNG.

DISCUSSION

We have shown previously that perinuclear localization of MT-1 mRNA and its association with the cytoskeleton is a prerequisite for subsequent localization of the MT-1 protein within the cell. Furthermore, this prior localization of the mRNA is necessary for the redistribution of MT-1 protein into the nucleus during the early S-phase of the cell cycle [14]. The present data show that loss of MT-1 mRNA localization has a major functional impact, namely on cell susceptibility to stress, on protection of DNA from damage and on apoptosis.

Cytotoxicity studies showed that MTMT cells, expressing the native MT-1 gene, were more resistant to exposure to heavy metals and oxidants than the MTGSH cells, in which MT 3′-UTR had been replaced with that of glutathione peroxidase; these latter cells were themselves more resistant than both IDIGSH cells and parental CHO cells. These data show that increased expression of MT-1 was associated with increased protection against oxidants and cadmium, and, furthermore, this effect was significantly greater when the MT-1 mRNA was correctly targeted in the cell. Thus MT-1 mRNA localization and the subsequent MT-1 protein distribution [14] appear critical for the protein's function. Overall, the data support the hypothesis that MT-1 has an important role in protecting the cell against oxidative stress.

In order to relate these stress responses to a possible role of MT in the nucleus, DNA damage was assessed in both exponentially growing cells and cells synchronized at the early S-phase of their cell cycle. The MTMT cell line exhibited less DNA damage after exposure to oxidants and alkylating agent than the three other cell lines in both synchronized and unsynchronized cell populations. Since MT-1 is effectively redistributed to the nucleus in the MTMT cells, but not in MTGSH cells during S-phase, these data indicate that nuclear localized MT in the nucleus has a role to play in the nucleus in protection of DNA against damage. Likewise, there was an indication that MTMT cells were undergoing less apoptotic death after exposure to UVC light and alkylating agent than MTGSH, CHO and IDIGSH cells. Therefore MT-1 protein plays a role in protecting the cell against oxidative stress and DNA damage, and also influences apoptotic cell death. These results, combined with data obtained from the study on MT mRNA localization [14], argue that a loss of MT-1 mRNA localization, and therefore a loss of protein localization, is accompanied by increased susceptibility to oxidative stress, DNA damage and apoptotic death, and they support the hypothesis that nuclear MT has an important role in protection of DNA [12].

The reduced protection afforded by MT-1 in cells where it is not effectively redistributed into the nucleus suggests that nuclear MT-1 is important in protecting cells from oxidative stress. This hypothesis is supported by the observed increase in DNA damage and apoptosis in these cells. The importance of nuclear MT-1 is supported further by work performed on differentiating myotubes, which, unlike myoblasts, do not express MT in the nucleus and have been shown to be more sensitive to apoptosis than myoblasts [25]. However, previous work with cells transfected with a modified MT-1 gene construct so that the MT-1 is effectively only present in the nucleus [12] showed that, when MT-1 was exclusively nuclear, it provided no protection of the cell against radical oxygen species as a result of exposure to t-butyl hydroperoxide; in the case of the MT-null fibroblasts transfected with MT-1 featuring an added nuclear localization signal [12], it is unlikely that there was shuttling of MT protein between nucleus and cytoplasm. In contrast, in the present work the protective effects of MT-1 are most effective in cells, which show the capacity to redistribute MT-1 into the nucleus. Taken together, the present work and the previous observations of Woo and Lazo [12] suggest that the protective role of MT-1 requires that the protein redistributes between nuclear and cytoplasmic compartments. The reason for this is unknown. However, it has recently been observed that the nuclear localization of MT-1 occurs simultaneously with an increase in zinc levels in the nucleus during the G_1-to-S-phase transition of the cell cycle [26]. In view of the known metal-binding properties of MT-1, it is likely that the redistribution of MT-1 is associated with a need for zinc in the nucleus, and that this is one possible mechanism through which MT-1 could exert its protective effects.

In conclusion, the present data provide the first evidence that perinuclear mRNA localization has a functional role to play in the cell. Localization promotes nuclear MT-1 import [14], which, in turn, is a prerequisite for protection of the cell against oxidative stress and DNA damage. Our hypothesis is that the localized synthesis of MT facilitates the transport of MT-1 between cytoplasm and nucleus, and that this is important for protecting the cell against oxidative stress, DNA damage and apoptotic cell death. Other proteins become localized in the nucleus in a cell-cycle-specific manner, but it is not known whether these events are also dependent on mRNA localization. Further research is required to determine whether mRNA localization plays a role in the nuclear import of these other proteins. However, several mRNAs coding for proteins that are imported into the nucleus after synthesis (transcription factors c-Myc and c-Fos, ribosomal proteins) are found localized in the perinuclear cytoplasm and/or are associated with the cytoskeleton [9,27,28]; furthermore, in the case of c-Myc and c-Fos mRNAs, this targeting is dependent on 3′-UTR sequences ([6,9] and G. Dalgleish, J.-L. Veyrune, J.-M. Blanchard and J. E. Hesketh, unpublished work). On the basis of such data, it is likely that the targeted, local synthesis of c-Myc and c-Fos is important for efficient import of the proteins into the nucleus throughout the cell cycle. Thus the targeting of mRNAs to provide perinuclear protein synthesis for subsequent protein import appears not to be unique for MT-1, but also occurs for several other nuclear proteins, including some key transcription factors. However, the generality of the mechanism remains to be determined.

This work was supported by the Scottish Environment and Rural Affairs Department (SERAD). M.L.-M. received a scholarship from the Boyd Orr Research Consortium.

REFERENCES

1 Blobel, G. and Dobberstein, R. (1975) Transfer of proteins across membranes. Presence of proteolytically processed and unprocessed nascent immunoglobin light chains on membrane-bound ribosomes of murine myeloma. J. Cell Biol. **67**, 835–851
2 Kurzchalia, T. V., Wiedmann, M. and Girshovich, A. S. (1986) The signal sequence of nascent preprolactin interacts with the 54 kDa polypeptide of the signal recognition particle. Nature (London) **320**, 634–636
3 Silver, P. A. (1991) How proteins enter the nucleus. Cell **64**, 489–497
4 Jansen, R.-P. (1999) RNA–cytoskeletal associations. FASEB J. **13**, 455–466
5 Hesketh, J. E. (1996) Sorting of mRNAs in the cytoplasm: mRNA localization and the cytoskeleton. Exp. Cell Res. **225**, 219–236

6 Veyrune, J.-L., Campbell, G. P., Wiseman, J., Blanchard, J.-M. and Hesketh, J. E. (1996) A localization signal in the 3′untranslated region of *c-myc* mRNA targets *c-myc* mRNA and β-globin reporter sequences to the perinuclear cytoplasm and cytoskeletal-bound polysomes. J. Cell Sci. **109**, 1185–1194

7 Bassell, G. J., Powers, C. M., Taneja, K. L. and Singer, R. H. (1994) Single mRNAs visualized by ultrastructural *in situ* hybridization are principally localized at actin filament intersections in fibroblasts. J. Cell Biol. **126**, 863–876

8 Taneja, K. L., Lifshitz, L. M., Fay, F. S. and Singer, R. H. (1992) Poly(A) RNA codistribution with microfilaments: evaluation by *in situ* hybridization and quantitative digital imaging microscopy. J. Cell Biol. **119**, 1245–1260

9 Hesketh, J., Campbell, G., Piechaczyk, M. and Blanchard, J.-M. (1994) Targeting of c-*myc* and β-globin coding sequences to cytoskeletal-bound polysomes by c-*myc* 3′ untranslated region. Biochem. J. **298**, 143–148

10 Mahon, P., Partridge, K., Beattie, J., Glover, L. A. and Hesketh, J. (1997) The 3′untranslated region plays a role in the targeting of metallothionein-1 mRNA to the perinuclear cytoplasm and cytoskeletal-bound polysomes. Biochim. Biophys. Acta **1358**, 153–162

11 Tsujikawa, K., Imai, T., Kakutani, M., Kayamori, Y., Mimura, Y., Otaki, N., Kimura, M., Fukuyama, R. and Shimizu, N. (1991) Localization of metallothionein in nuclei of growing primary cultured adult rat hepatocytes. FEBS Lett. **283**, 239–242

12 Woo, E. S. and Lazo, J. S. (1997) Nucleocytoplasmic functionality of metallothionein. Cancer Res. **57**, 4236–4241

13 Panemangalore, M., Banerjee, D., Onosaka, S. and Cherian, M. G. (1983) Changes in the intracellular accumulation and distribution of metallothionein in rat liver and kidney during postnatal development. Dev. Biol. **97**, 95–102

14 Levadoux, M., Mahon, C., Beattie, J. H., Wallace, H. M. and Hesketh, J. E. (1999) Nuclear import of metallothionein requires its mRNA to be associated with the perinuclear cytoskeleton. J. Biol. Chem. **274**, 34961–34966

15 Miles, A. T., Hawksworth, G. M., Beattie, J. H. and Rodilla, V. (2000) Induction, regulation, degradation and biological significance of mammalian metallothioneins. Crit. Rev. Biochem. Mol. Biol. **35**, 35–70

16 Campbell, G. P. and Hesketh, J. E. (1996) Distribution of glutathione peroxidase mRNAs between free and cytoskeletal-bound polysomes in H4 hepatoma cells. Biochem. Soc. Trans. **24**, 189S

17 Mahon, P., Beattie, J., Glover, L. A. and Hesketh, J. (1995) Localization of metallothionein isoform mRNAs in rat hepatoma (H4) cells. FEBS Lett. **373**, 76–80

18 Bermano, G., Arthur, J. R. and Hesketh, J. E. (1996) Role of the 3′UTR in the regulation of cytosolic GSHPx and phospholipid-hydroperoxide GSHPx gene expression by selenium supply. Biochem. J. **320**, 891–895

19 Mosmann, T. (1983) Rapid colorimetric assay for cellular growth and survival: application to proliferation and cytotoxicity assays. J. Immunol. Methods **65**, 55–63

20 Collins, A. R., Ma, A. G. and Duthie, S. J. (1995) The kinetics of repair of oxidative DNA damage (strand breaks and oxidized pyrimidine dimers) in human cells. Mutat. Res. **336**, 69–77

21 Zheng, H., Liu, J., Liu, Y. and Klaassen, C. D. (1996) Hepatocytes from metallothionein-I and -II knock-out mice are sensitive to cadmium- and *tert*-butyl hydroperoxide-induced cytotoxicity. Toxicol. Lett. **87**, 139–145

22 Wyllie, A. H. (1980) Glucocorticoid-induced thymocytes apoptosis is associated with endogenous endonuclease activation. Nature (London) **284**, 555–556

23 Nicoletti, I., Migliorati, G., Pagliacci, M. C., Grignani, F. and Riccardi, C. (1991) A rapid and simple method for measuring thymocyte apoptosis by propidium iodide staining and flow cytometry. J. Immunol. Methods **139**, 271–279

24 Horvathova, E., Slamenova, D., Hlincikova, L., Mandal, T. K., Gabelova, A. and Collins, A. R. (1998) The nature and origin of DNA single strand breaks determined with the comet assay. Mutat. Res. **409**, 163–171

25 Apostolova, M. D., Ivanova, I. A. and Cherian, M. G. (1999) Metallothionein and apoptosis during differentiation of myoblasts to myotubes: protection against free radical toxicity. Toxicol. Appl. Pharmacol. **159**, 175–184

26 Apostolova, M. D., Ivanova, I. A. and Cherian, M. G. (2000) Signal transduction pathways, and nuclear translocation of zinc and metallothionein during differentiation of myoblasts. Biochem. Cell. Biol. **78**, 27–37

27 Hovland, R., Campbell, G., Pryme, I. and Hesketh, J. (1995) The mRNAs for cyclin A, *c-myc* and ribosomal proteins L4 and S6 are associated with cytoskeletal-bound polysomes in HepG2 cells. Biochem. J. **310**, 193–196

28 Bird, R. C. and Sells, B. H. (1986) Cytoskeleton involvement in the distribution of mRNP complexes and small cytoplasmic RNAs. Biochim. Biophys. Acta **868**, 215–225

Received 26 October 2000/18 December 2000; accepted 31 January 2001